ISSN:1687-1006

The Egyptian International Journal of Engineering Sciences and Technology

Vol. 31 (2020) 51–61

https://eijest.journals.ekb.eg/

Numerical investigation of corrugated plate interceptor efficiency and its related parameters

Mohamed H. Gobran, Radwan M. Kamal , Mohamed Hassanein*, Mohammed A. Boraey

Department of mechanical power engineering, faculty of engineering, Zagazig University, 44519 Zagazig, Egypt.

ARTICLE INFO

Keywords:

Water Treatment; CPI
Oil Separation
Produced Water
Particle Tracking
Numerical Modeling
Two-phase Flow.

ABSTRACT

Produced water quality has become an increasingly large area of concern for the oil production industry. A great deal of scientific research has been carried out to determine the consequences of exposure of produced water on the environment. Some of this research has given alarming results. Also, some of the toxic components in produced water may cause irreversible damage to the surrounding environment. Because of this potential risk, very considerable efforts oil separation technologies and researches are being expended. The corrugated plate interceptor is an efficient technique used for oil/water separation from 30 µm to150µm. In the present work, a two-dimensional mathematical model has been developed to investigate the effect of different Reynolds numbers (Re) and droplet diameter (d) on the corrugated plate interceptor performance (efficiency and catch length). The properties of water flow are solved using continuous phase governing equations (Eulerian approach). After that discrete phase equation of motion is solved, through the water moving stream (Lagrangian approach). The governing equations were solved between two corrugated plates using a finite volume FLUENT solver. The investigation showed that the separation efficiency is inversely proportional to the Reynolds number and directly proportional to the oil droplet diameter. It also shows that when the Reynolds number is less than 10 and the droplet diameter great than 30 µm the separation efficiency is almost 98%.

1. Introduction

Produced water or oilfield brine is the waste-water that represents more than 80% of the liquid waste in the modern oil and gas industry and may reach 95% in aging oilfields with volumetric ratio3:1 [Igunnu and Chen 2012] [1]. About 250 million barrels per day of produced water is separated from oil/gas it is treated (15 mg/L to 50 mg/L oil still exists) and then discharged to surface water or re-injected for either reservoir pressure maintenance or disposal [Igunnu and Chen 2012] [1].Recycling or re-use of produced water is an ongoing area of focused research and development that has equipped the oil and gas industries [Wells 2009] [2]. Since the total disposal costs are $0.30/bbl to $105.00/bbl according to the technique used. [Drewes et al 2009] [3].Oil-water separation technologies can be classified into two main types; gravity and non-gravity based separation technologies. The most common and widely used non-gravity based separation technologies are Hydro cyclones, Filtration ....etc. Gravity separation technologies rely on the fact that the specific gravity of oil is less than that of water. Gravity separation technologies can broadly be

* Corresponding author. Tel. +201069684894
E-mail address: m_hasanin24@yhaoo.com .

divided into two main categories; those that operate with and without the assistance of gas in the flotation process. Non-gas-assisted flotation includes gravity separation tanks and corrugated plate interceptors [Atarah 2011] [4].

Corrugated Plats Oil Interceptor (CPI) is one of the most efficient techniques which used in de-oiling produced water. All vendors produced CPI with different geometries and configurations to get the best separation efficiency[Ciarapica and Giacchetta 2003][5].Their advantages include high separation efficiency, compact construction, minimum maintenance and operation costs and no energy consumption except water pumping.

2. Corrugated Plats Oil Interceptor (CPI)

The CPI Oil Separator is a compact unit as shown inFig. 1. Its components are1-Inlet pipe, 2-sedimentation chamber, 3-weir plate, 4-corrugated-plate packs and 5-outlet pipe.

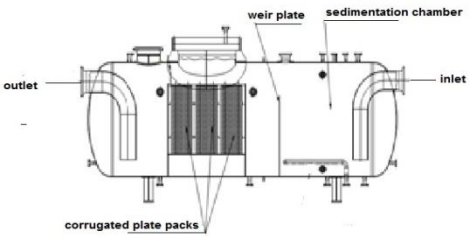

Fig. 1: Schematic drawing of CPI apparatus

The plate pack as shown in Fig. 2 is consists of multiple corrugated parallel plates designed to allow for oil droplet coalescence and separation. Therefore, small oil droplets have only a short distance to rise and collide with other droplets to form a buoyant film on the underside of the plate.

In the apexes of the corrugation ridges, many holes (15 mm diameter) are bored as shown in Fig. 2. These holes allow the oil collected in the apexes of the ridges to move upward and reach the oil collection layer.

Fig.2: Photo of corrugated plates.

3. previous researches

Yayla et al 2017[6] simulated the flow in a 2-D computational model which was developed to investigate the effect of the Reynolds number and plate-hole shape on the separation efficiency. Spacing between plates was taken as 12 mm and the fluid mixture's Re was varied between 5 and 45. The study reported that separation efficiency is inversely proportional to the Reynolds number. In this study, the Reynolds number variation was based only on velocity (v) variation, while the spacing (h) remains fixed (12 mm). Also, the effect of oil droplet volume was not considered.

Ivanenko et al 2010[7] used the "Flow Vision" software to solve the flow between plates. Their numerical experiment results show that the degree of purification depends on the drop size. The actual efficiency of oil separation from water has been investigated experimentally. They prepared an emulsion with an average size of oil drops of 20 μm and made it flow into the package of corrugated plates. The gap between the plates was 6 mm, the number of channels was 12, and the number of plates was 13. The package of the plates was placed into a rectangular vessel. According to their experiment results, the velocity of emulsion in the channels controls the gravitational separation time, and the process of inertia. The study shows good agreement between the mathematical model and the experimental results.

Ostrovski et al 2003[8] studied the gravity separation of particles in flow between flat channels. The particle size distribution and the flow velocity field were studied. The inertial forces are extremely weak, but very necessary to determine limiting values of the layer thickness and the average flow velocity. In the all of study cases, the equation of motion of a particle can be represented for the Stokes flow and the transverse Saffman force. In this study, the spacing between plates was varied from 6 mm to 20 mm. The examined inclined angle was 45 or 60 degrees and separating oil droplets diameters from 60 to150 microns.

Abdulkadir et al 2010[9] numerically analyzed the characteristics of fluid flow in a cylindrical horizontal separator with different velocities and droplet diameters. They use the Eulerian model for multi-phase flow in the software Fluent 6.2, and GAMBIT2.2, taking into consideration turbulence effects using the k-ε model. The results were that the

separation efficiency is inversely proportional to the mixture velocity. The oil droplet diameter size has a great effect on the oil separation efficiency. The simulations show that CFD can be a useful tool in studying a horizontal oil-water separator.

Chen et al 2015[10] numerically studied the multi-phase flow based on the Euler approach and k- ε turbulence model to obtain a comprehensive understanding of the internal flow within the separator. Orthogonal array experiments were done to select the optimal value ranges of the separator's various structural parameters. The Study reported that the separation efficiency of the inclined separator was higher than that of the conventional horizontal separator under the same conditions. The oil/water separation efficiency at optimum condition was 95%, where the experiment efficiency was 4.996% smaller than theoretical.

4. CFD Setup

4.1. Computational domain

A CPI battery consisting of 13 corrugated profiled plates which are arranged to make 12 channels. Single-channel between two plat configurations is illustrated in Fig. 3.

Fig. 3: real photo of computational domain.

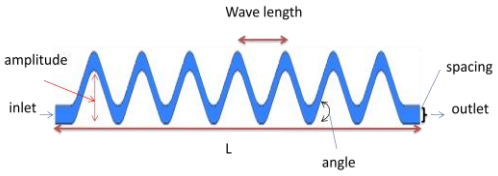

Fig. 4: schematic of computational domain.

The plat length is (L) 625 mm, the amplitude is 22 mm, the wavelength is 70 mm, the upper bending radius is 11 mm, and the lower bending radius is 14 mm.As shown in Fig. 5

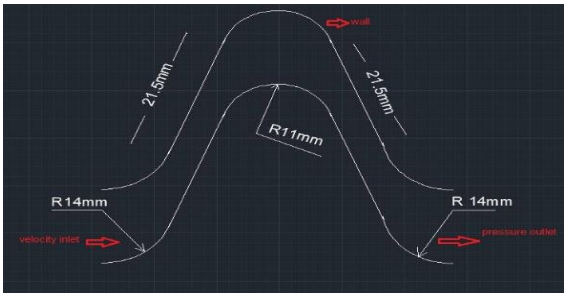

Fig. 5: Dimensions of the single corrugation profile

4.2. Computational mesh creation

The number of nodes for one of the present cases study is 123,350 of unstructured mesh

Fig. 6. Mesh description is Quad/Tri and mesh type is map as reported in Gambit. Also, one of mesh important quality parameters is Equi-size-skew that equal 1.345810-10 as reported in Gambit mesh quality report.

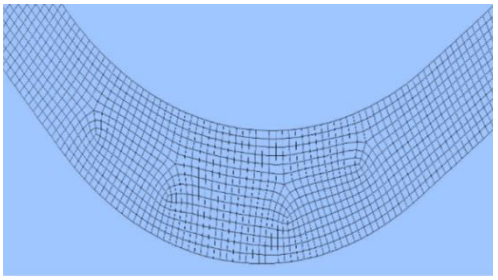

Fig. 6: focused view one of the present meshes.

The mesh-sensitivity was accomplished by calculating the separation efficiency-Reynolds number relation at a different number of cells

Fig. 7 shows that.

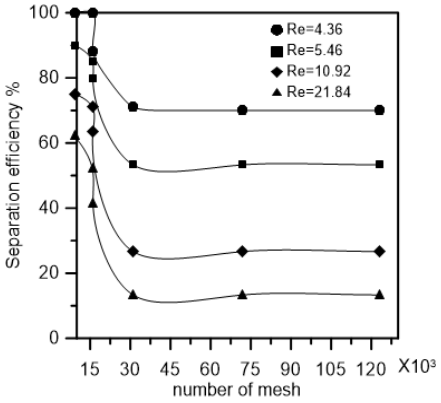

Fig. 7: mesh independence test.

Every case has a different mesh because the spacing between plates changes the face geometry.

4.3. Boundary condition (BC)

Inlet BC is set as inlet velocity. A uniform velocity normal to the entrance plane is considered.

Outlet BC is set as outflow. In ANSYS FLUENToutflow boundary conditions are used to model flow exits where the details of the flow velocity and pressure are not known prior to solving the flow problem. Wall BC set as with no slip. The particles are trapped when they reach the wall.Table 1 shows the base case value relative to parametric parameters value.

Table 1: base case value relative to parametric parameters value

	Parametric parameters	Base case
inlet	Velocity varied(0.5 cm/s to 7 cm/s)	1.5 cm/s
Out let	Set as outlet flow	
wall	No slip – trapped particles	
Particle numbers	Depend in the inlet surface injection (120 to one).	70
Particle diameter	Varied from 10 to 60 microns	30 microns
Plate length	625 mm	625 mm

5. Separation mechanism

The oil/water mixture enters the CPI through the plate pack section of the separator as shown in Fig. 8. The oil droplet moves upward before it contacts the next corrugated plate from holes at the upper side of the plate as shown in Fig. 9. and when it touches a corrugated plate it is trapped or separated.

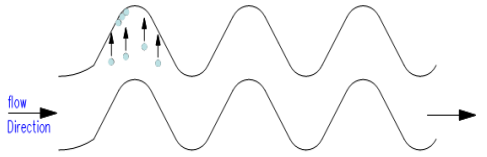

Fig. 8: Oil droplets rise.

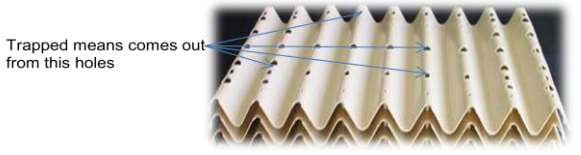

Fig. 9: holes which droplets come out from it.

This is because when the droplet adheres to the underside of the corrugated plate and moves along the plate to the apex of the corrugation ridge as shown in

Fig. 10. Boreholes in the apices of the corrugation ridges (diameter 15 mm), allow the oil collected in the apices of the ridges to move upward and reach the oilcollection layer. This makes the CPIis more efficient than API separation tanks.

Fig. 10: Oil layer at apex

6. Mathematical Modeling

6.1. Stokes law

TO simulate the separation process for an emulsion of two liquids flows between two channels and one of the liquids is heavier than the other, the differences in densities of the two liquids cause droplets to rise or fall by their buoyancy as shown in Fig. 11.

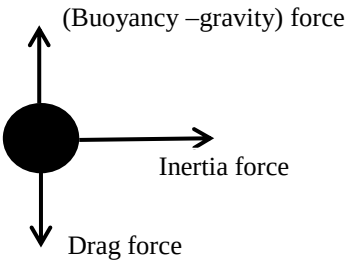

Fig. 11: Forces on oil droplet.

The viscous force acting on anoil droplet or particle is directly proportional to the following parameters [Concha and Fernando 2014] [12]:

- the radius of the droplet.
- coefficient of viscosity.
- the velocity of the droplet.

Mathematically, this is represented as
F α μa rbvc

Now let us evaluate the values of a, b and c.
Substituting the proportionality sign with an equality sign, we get

F = k μa rbvc (1)

Here, k is the constant of proportionality which is a numerical value and has no dimensions.
Writing the dimensions of parameters on either side of equation (1), we get

[MLT–2] = [ML–1T–1]a [L]b [LT-1]c

Simplifying the above equation, we get

[MLT–2] = Ma * L–a+b+c * T–a–c (2)

According to classical mechanics, mass, length and time are independent entities.
Equating the superscripts of mass, length and time respectively from equation (2), we get

a = 1 (3)

–a + b + c = 1 (4)

–a –c = 2 or a + c = 2 (5)

Substituting (3) in (5), we get

1 + c = 2

c = 1 (6)

Substituting the value of (3) & (6) in (4), we get

–1 + b + 1 = 1

b = 1 (7)

Substituting the value of (3), (6) and (7) in (1), we get

F=kμrv

The value of k for a spherical body was experimentally obtained as 6π Therefore; the viscous force (drag force) on a spherical body falling through a liquid is given by the equation

F=6πμrv = 3πμdv

Bouncy force – gravity force = drag force

Density of water* volume of the droplet – density of oil droplet * volume of the droplet = 3πμdv

ρw*Vp – ρo*Vp = 3πμdpv

(π/6)Δρ*dp3*g=3πμdpv

V = (Δρ*dp2*g)/ 18μ

This mechanism of separating liquids by gravity is called Stokes Settling law, which can be written as below:

$$V_r = 5.6 \, X \, 10^{-7} \, \frac{(\Delta S.G.)d^2}{\mu} \qquad (1)$$

6.2. Governing equations

The equation for conservation of mass, or continuity equation, can be written as follows:

$$\frac{\partial \rho}{\partial t} + \nabla \cdot (\rho \vec{v}) = S_m \qquad (2)$$

Equation (2) is the general form of the mass conservation equation and is valid for incompressible as well as compressible flows. The source S_m is the mass added to the continuous phase from the dispersed second phase (e.g., due to vaporization of liquid droplets) and any user-defined sources (fluent guide) [11].

Conservation of momentum in an inertial (non-accelerating) reference frame is described by:

$$\frac{\partial}{\partial t}(\rho \vec{v}) + \nabla \cdot (\rho \vec{v} \vec{v}) = -\nabla p + \nabla \cdot (\bar{\bar{\tau}}) + \rho \vec{g} + \vec{F} \qquad (3)$$

Where p is the static pressure, $\bar{\bar{\tau}}$ is the stress tensor (described below), and $\rho \vec{g}$ and $\vec{F}$ are the gravitational body force and external body forces (e.g., that arise from interaction with the dispersed phase), respectively.

The stress tensor $\bar{\bar{\tau}}$ is given by:

$$\bar{\bar{\tau}} = \mu \left[(\nabla \vec{v} + \nabla \vec{v}^{\,T}) - \frac{2}{3} \nabla \cdot \vec{v} I \right] \qquad (4)$$

Where μ is the molecular viscosity, I is the unit tensor, and the second term on the right hand side is the effect of volume dilation.

Discrete Phase Model: This model used for a very low volume fraction and the dispersed phase must be found at less than 10–12% (fluent guide) [11]. The trajectory of a particle can be obtained by integrating its equation of motion. From Newton's second law of motion principle, the particle equation of motion per unit mass of the particle is written as;

$$\frac{d\vec{V}_p}{dt} = \vec{F}_D + \frac{\vec{g}(\rho_p - \rho)}{\partial X_i} + \vec{F} \quad (4)$$

Where;

$$\vec{F}_D = \frac{18\,\mu C_D \mathrm{Re}\,r}{24\rho_p d_p^2}\left(\vec{V} - \vec{V}_p\right)$$: Drag /unit mass

$$\mathrm{Re}_r = \frac{\rho\, d_p \left|\vec{V}_p - \vec{V}\right|}{\mu}$$

Drag force coefficient (CD), [Schiller and Naumann 1935] [13] suggest the following formulation for CD for stokes flow or creeping flow but for higher values of Re there is a different approaches have been reported in Table 2.

Table 2: CD[Schiller and Naumann 1935]

CD =	24 / Re	If Re < 0.5
	24 (1 + 0.15 Re0.678) / Re	If 0.5 < Re < 1000
	0.44	If Re > 1000

Similarly, [Morsi and Alexander 1972][14] proposed a more complete approach in the form of CD

CD = a1 + a2/Re + a3/Re2

With the coefficients a1, a2 and a3 show in the Table 3for Re ranges.

Table 3: values of a1, a2, a3.

Rang	a1	a2	a3
Re < 0.1	0	24	0
0.1 < Re < 1	3.69	22.73	0.0903
1 < Re < 10	1.22	29.1667	-3.889
10 < Re < 100	0.6167	46.5	-116.62
100 < Re < 1000	0.3644	98.33	-2778

In this model the exchanging of momentum, mass, and energy between phases is available. The Euler-Lagrange approach was considered. The particle force balance was considered to get the equations of motion for particles. The trajectory of a droplet was predicted by integrating the force balance on it.Navier-Stokes equations have been used to solve the continuous phase equations. The dispersed phase was been solved by tracking a large number of particles or droplets through the calculated flow field.

7. Results and discussion

7.1. Cases for the flow Reynolds number

By tuning different combination of inlet velocity (V) and plates spacing length (h) are assumed to obtain various Reynolds numbers ($Re_{(flow)} = (\rho_w - \rho_o)*v*h/\mu_{mix}$). As shown inTable 4.

Table 4: table of some cases for velocity inlet variation

Velocity (v) m/s	Spacing (h) mm	Re
0.005	0.01	10.9235
0.01	0.01	21.847
0.015	0.01	32.7705
0.01	0.005	10.9235
0.02	0.005	21.847
0.03	0.005	32.7705
0.015	0.015	49.15575
0.02	0.015	65.541
0.03	0.015	98.3115

The developed model solves the continuous phase as water and a dispersed phase as oil. Where, the oil droplets injected from the inlet surface through the continuous phase with the same velocity.

Also, the droplet diameter is changed from 10 to 60 µm, to study the effect of droplet diameter on both separation efficiency and catch length.

7.2. separation efficiency definition

The oil droplets are uniformly injected from the inlet surface, depending on the number of cells, in cases of a separation efficiency study. The oil droplets have the same diameter for every single case. The separation efficiency is calculated by dividing the number of trapped particles as seen in Fig.13 and Fig. 16 on the total number of injected particles at inlet.

$$\eta = \frac{no.trapped\ particles}{no.total\ partucle} \quad (5)$$

For droplet size distribution the separation efficiency by the following equation,

$$\eta = \frac{oil\ concentration \text{ at the outlet}}{\text{oil concentration at input}} \qquad (6)$$

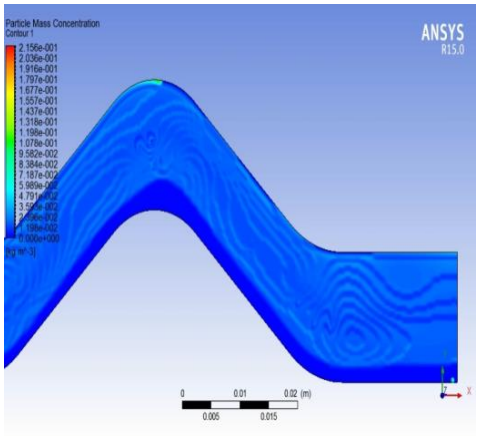

Fig. 12: oil layer concentration.

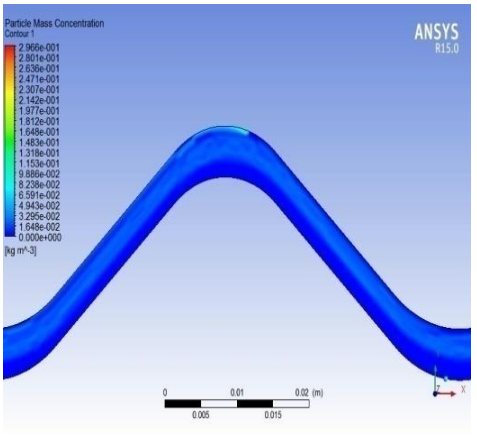

Fig.13: oil layer concentration.

7.3. Validation

To check the validity of the present work model, some of the results were compared with the work byIvanenkoet al.2010 with the same geometry configuration for the plates and the same oil droplet diameter (33 microns).

Fig. 14 illustrates this comparison. It was noted that there is a great agreement especially for the experimental results of Ivanenko.

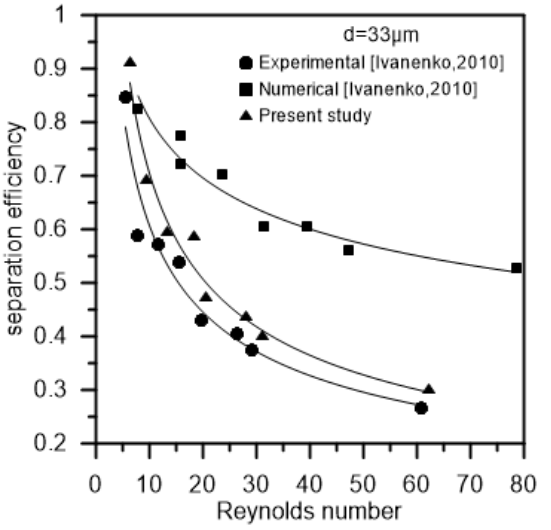

Fig. 14: results comparison with the work by Ivanenko et al., 2010.

7.4. Separation efficiency study

The separation efficiency against Reynolds number at different droplet diameters shown in

Fig. 15. The higher was the Reynolds number, the lower the separation efficiency and vice versa. Also as the droplet diameter increases the separation efficiency increases because of higher buoyancy. According to Stokes law where water is heavier than oil.

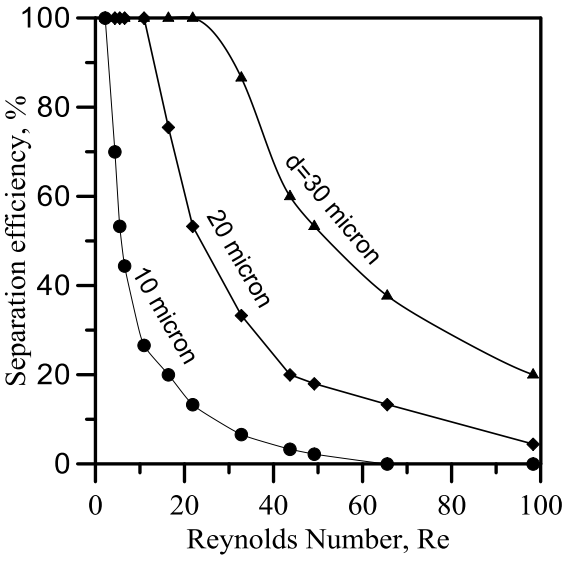

Fig. 15: The separation efficiency Vs. Re at different droplet diameter

7.5. Catch length

In the case of catch length, a single droplet is injected from the inlet near to the lower plate edge which is been considers as the worthiest case, Fig. 16.

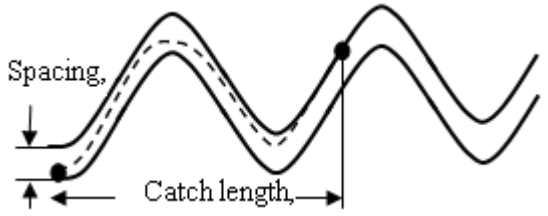

Fig. 16: the catch length for single droplet.

The variation of catch length with the droplet diameter at different values of Reynolds number is shown in

Fig. 18. It is noticed that for all Reynolds numbers, as the droplet diameter increases, the catch length decreases.

The residence time

Fig.17can be then calculated by dividing the catch lengthover the flow velocity. The diameter of the oil drop has a significant impact on buoyancy which is the driving force behind the separation process.

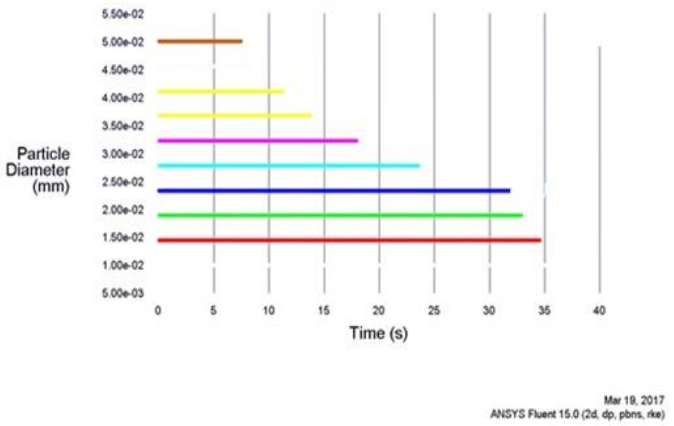

Fig.17: The residence time for different droplets.

The catch length is an indicator of separation efficiency. The lower the length, the lower the residence time will be. That will lead to smaller apparatus and lower initial cost.

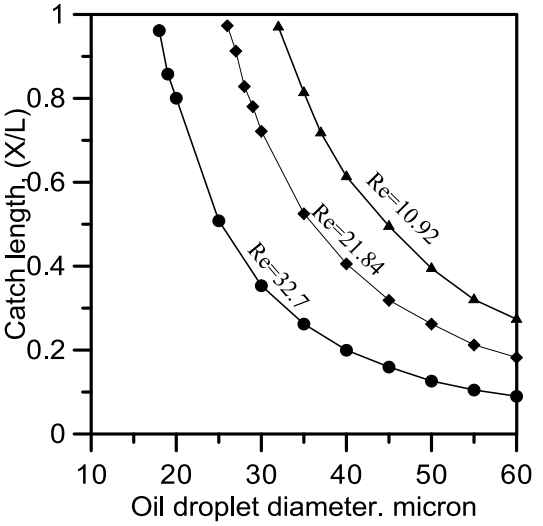

Fig. 18: The droplet diameter Vs. catch lengths ratio at different Re.

The particle tracking for the 10-micron droplet diameter is shown in (Fig. 19-a) which illustrates that the oil is not fully-trapped and separation efficiency is low. Also, the oil is fully trapped at the eighth peak for the 20-micron droplet, as shown in (Fig. 19-b) which means that the separation efficiency increases. Finally, the oil is fully trapped at the fourth peak for the 30-micron droplet, shown in Fig. Fig. 19-c, that means that the separation efficiency increases more.

Another technique is performed. Only one oil-droplet is injected in the water flow as shown in Fig. 20. This is to investigate the catch length (residence distance) of the oil droplet.

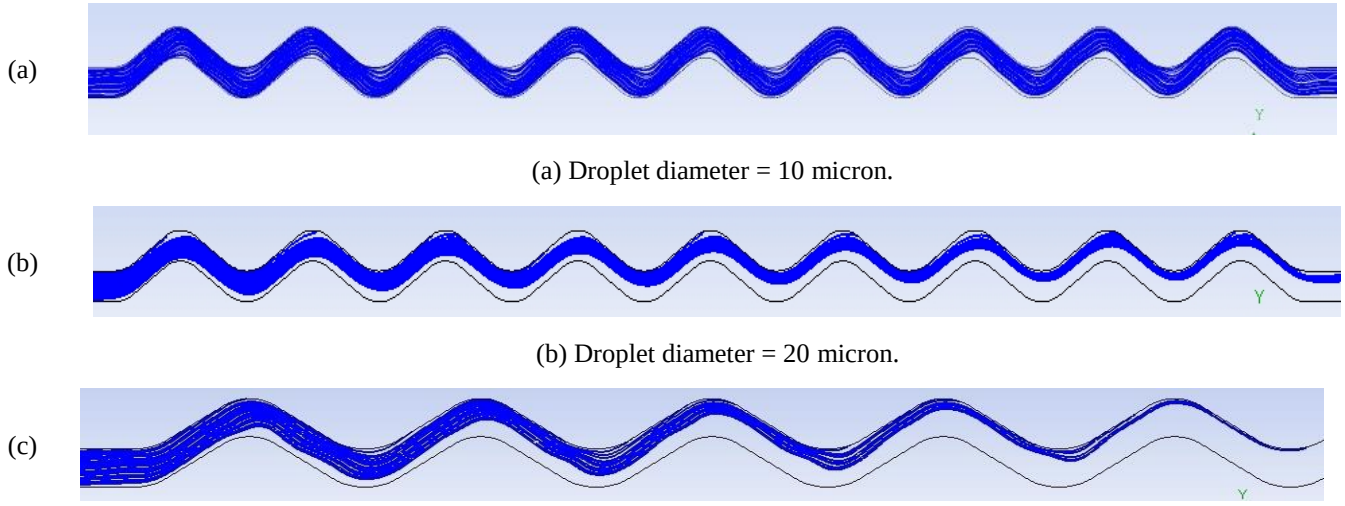

(a) Droplet diameter = 10 micron.

(b) Droplet diameter = 20 micron.

(c) Droplet diameter = 30 micron.

Fig. 19: Particle tracking of oil droplets with different droplet diameter, spacing between plates = 15 mm, and the flow velocity = 0.005 m/s.

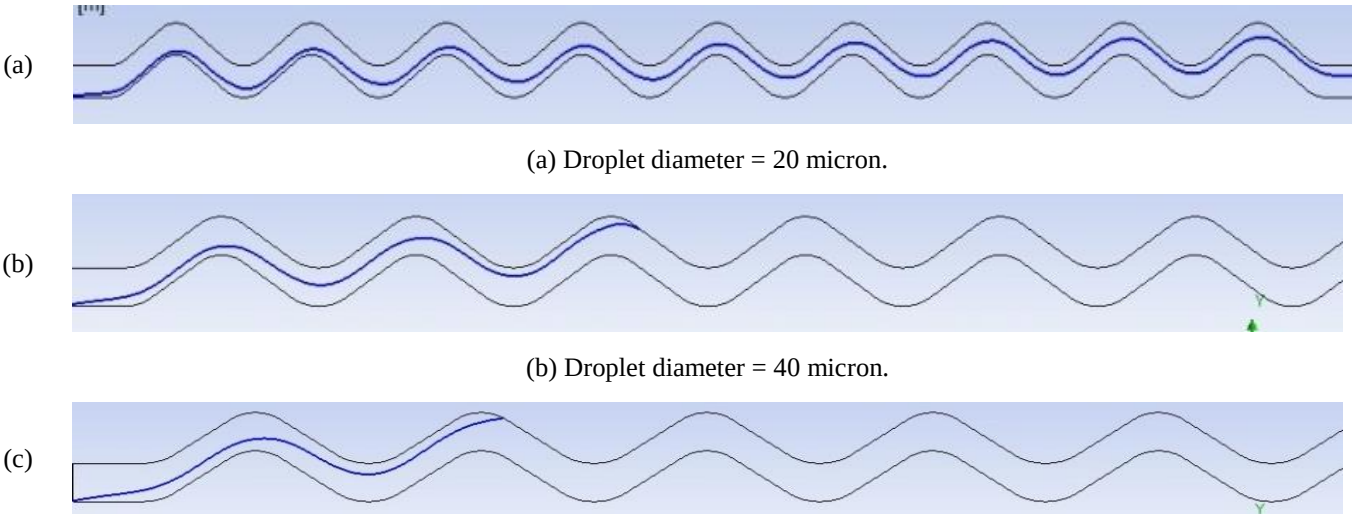

(a) Droplet diameter = 20 micron.

(b) Droplet diameter = 40 micron.

(c) Droplet diameter = 50 micron.

Fig. 20: Particle tracking of single oil droplet with different droplet diameter, spacing between plates = 15 mm, and the flow velocity = 0.005 m/s.

The catch length and separation efficiency are affected by Re regardless however it is obtained, by varying velocity or spacing between plates as shown in Fig. 21 and Fig. 22.

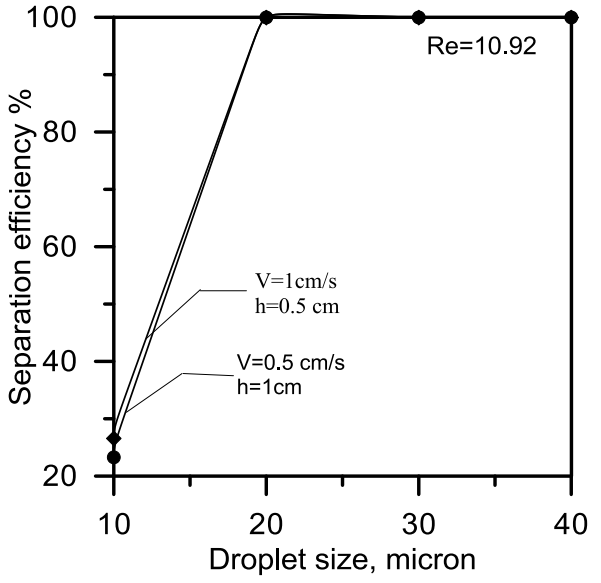

Fig. 21: different combination from velocity(v) and spacing (h) to get same Re Vs. separation efficiency

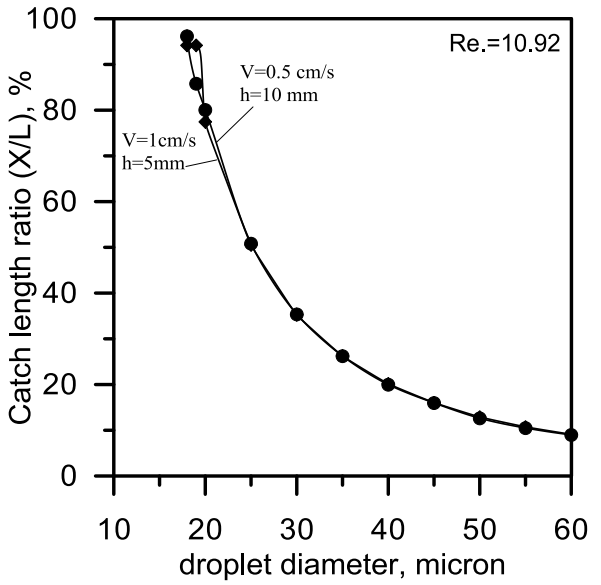

Fig. 22: different combination from velocity(v) and spacing (h) to get same Re Vs. catch length

8. conclusion

1- Fluent code is valid for modeling the oil separation in produced water treatment.
2- Decreasing Re leads to increasing separation efficiency and vice versa.
3- Increasing the droplet diameter increases the separation efficiency and decreases the catch length, vice versa.
4- Decreasing the catch length will lead to decreasing the residence time and vice versa.
5- When the plate spacing increases that leads to decreasing the separation efficiency and increasing both of catch length and residence time.
6- It is recommended that the water and oilmixture's entry speed should be 1.5 cm / s and the distance between the oil separator layers be 7 mm when the length of the plats is 590mm to improve the separation efficiency and to remove 30-micron droplets within approximately 36 seconds. This Optimizes operation conditions to reduce operation costs.

Nomenclature	
ρ	is the fluid density
p	the static pressure
d	Droplet Diameter, microns
V_r	Settling Velocity, m/s.
ΔS.G	Specific Gravity Difference between the Continuous and Dispersed Phases.
$\vec{F}$	Additional force per unit particle mass
$\vec{V}$	The fluid phase velocity
$\overrightarrow{V_p}$	The particle velocity
μ	The molecular viscosity of the fluid
ρ_p	The density of the particle

d_p	The particle diameter
C_D	The drag coefficient
Greek symbols	
η	separation efficiency
μ	Continuous Phase Viscosity, (cp)
Subscripts	
p	particle
Abbreviations	
CPI	Corrugated plate Inceptor

References

[1] E. T. Igunnu and G. Z. Chen, "Produced water treatment technologies," International Journal of Low-Carbon Technologies, vol. 9, pp. 157-177, 2012.

[2] G. WELLS, "MANAGEMENT OF PRODUCED WATER FROM OIL AND GAS WELLS."

[3] J. E. Drewes, T. Y. Cath, P. Xu, J. Graydon, J. Veil, and S. Snyder, "An integrated framework for treatment and management of produced water," RPSEA Project, pp. 07122-12, 2009.

[4] J. J. A. Atarah, "The use of flotation technology in produced water treatment in the oil & gas industry," University of Stavanger, Norway, 2011.

[5] F. Ciarapica and G. Giacchetta, "The treatment of produced water in offshore Rig: Comparison between Tradition Installations and Innovative Systems: 2003: The Fifth International Membrane Science & Technology Conference," University of New South Wales, 2003.

[6] S. Yayla, S. S. Ibrahim, and A. B. Olcay, "Numerical investigation of coalescing plate system to understand the separation of water and oil in water treatment plant of petroleum industry," Engineering Applications of Computational Fluid Mechanics, vol. 11, pp. 184-192, 2017.

[7] A. Y. Ivanenko, M. Yablokova, and S. Petrov, "Simulation of the separation of emulsified oil products from water in an apparatus with sinusoidal-profiled oleophilic plates," Theoretical Foundations of Chemical Engineering, vol. 44, pp. 729-741, 2010.

[8] G. Ostrovskii, "Theory of gravity separation of particles from liquid in cocurrent and countercurrent thin-layer settlers," Theoretical Foundations of Chemical Engineering, vol. 37, pp. 503-509, 2003.

[9] M. Abdulkadir and V. Hernandez-Perez, "The effect of mixture velocity and droplet diameter on oil-water separator using computational fluid dynamics (cfd)," World Academy of Science, Engineering and Technology, vol. 61, pp. 35-43, 2010.

[10] L. Chen, S. Wu, H. Lu, K. Huang, and L. Zhao, "Numerical simulation and structural optimization of the inclined oil/water separator," PloS one, vol. 10, p. e0124095, 2015.

[11] A. Fluent, "14.5, theory guide; ansys," Inc., Canonsburg, PA, 2012.

[12] Concha, Fernando. (2014). Sedimentation of Particulate Systems.10.1007/978-3-319-02484-4_4.

[13] Shiller, L. and Naumann, A. (1935) A Drag Coefficient Correlation. Zeitschrift des Vereins Deutscher Ingenieure, 77, 318-320.

[14] Morsi, S. A., & Alexander, A. J. (1972). An investigation of particle trajectories in two-phase flow systems. Journal of Fluid Mechanics, 55(02), 193.